Available online at www.sciencedirect.com
ScienceDirect
Ceramics International 34 (2008) 1335–1339
CERAMICS INTERNATIONAL
www.elsevier.com/locate/ceramint

Influences of La^{3+} and Er^{3+} on structure and properties of Bi_2O_3–B_2O_3 glass

Yin Cheng [a,*], Hanning Xiao [a,b], Wenming Guo [b]

[a] College of Materials Science and Engineering, Changsha University of Science & Technology, Changsha 410076, China
[b] College of Materials Science and Engineering, Hunan University, Changsha 410082, China

Received 13 November 2006; received in revised form 20 December 2006; accepted 20 March 2007
Available online 6 May 2007

Abstract

$Bi_2O_3{\cdot}2B_2O_3$ glasses doped with La_2O_3 and Er_2O_3 were prepared by the melting-quenching method with AR-grade oxides. IR analysis was used to investigate the glass network structure. The characteristic temperatures including the glass transition temperature (T_g), crystallization temperature (T_p), and melting temperature (T_m) were estimated by DSC. The coefficient of thermal expansion (α), mass density (D), and Vickers hardness (H_v) were also measured. The results show that the basic network structure of $Bi_2O_3{\cdot}2B_2O_3$ glasses doped with rare-earth oxides consists of chains composed of [BO_3], [BO_4], and [BiO_6] units. La_2O_3 and Er_2O_3 act as network modifiers. As the doping concentrations of the rare-earth oxides were increased, T_g increased and α decreased, indicating that a more rigid glass was obtained. Er_2O_3 reduces the melting temperature and prevents glass crystallization. La_2O_3 contributes to the improvement of the microhardness of $Bi_2O_3{\cdot}2B_2O_3$ glass.

Keywords: Thermal properties; Glasses; Rare-earth oxide; Glass structure; Vickers hardness

1. Introduction

Increasing attention has been focused on crystallized glasses containing nonlinear optical crystals because of the high potential of these glasses for use in applications such as laser hosts, tunable waveguides, tunable fiber gratings, and so on [1–3]. Recently, $BiBO_3$, a new metastable crystalline phase, was found to have a larger nonlinear optical coefficient than the nonlinear optical coefficients of other existing nonlinear optical materials; therefore, it is considered to be a new candidate for use as a nonlinear optical material [4,5]. However, the metastability of the $BiBO_3$ crystal and its low synthetic ratio prevent the applications of Bi_2O_3–B_2O_3 glass from being used widely. Rare-earth ions containing special 4f electrons that are capable of excitation can greatly improve the nonlinear optical properties of glasses; consequently, the use of these ions can contribute to the development of the applications of optical materials [6–8]. Studies on rare-earth ions doped in Bi_2O_3–B_2O_3 glass showed that the structure of the $BiBO_3$ crystal could be stabilized by substituting Gd^{3+} for Bi^{3+}, resulting in excellent nonlinear optical properties [9–11]. Glasses doped with Nd^{3+}, Er^{3+}, Sm^{3+}, and La^{3+} have also been reported and are regarded as excellent laser materials [12,13]. Although these glasses are considered to be promising materials for use in all-optical devices, it is required for them to possess high thermal stability, excellent surface polishing properties, high refractive index, etc. Therefore, it is necessary to clarify the relationship among the structural, thermodynamic, and physical properties of Bi_2O_3–B_2O_3 glass doped with rare-earth ions for gaining a better understanding of and forecasting the functional properties of bismuth borate glass. In this study, $Bi_2O_3{\cdot}2B_2O_3$ glass was used as the basic glass composition. The influences of La^{3+} and Er^{3+} on the structure and properties of Bi_2O_3–B_2O_3 glass were investigated.

2. Experiments

$Bi_2O_3{\cdot}2B_2O_3$ glasses doped with La_2O_3 and Er_2O_3 (L series and E series, respectively) were prepared by the conventional melting-quenching method with AR-grade Bi_2O_3, B_2O_3, La_2O_3, and Er_2O_3 used as raw materials. After homogenization, the samples were melted in the temperature range of 700–1000 °C, quenched in a graphite mould, and crystallized at

* Corresponding author.
E-mail address: zjbcy@126.com (Y. Cheng).

0272-8842/$34.00
doi:10.1016/j.ceramint.2007.03.028

Table 1
Concentration of rare-earth oxide in the samples (mol%)

	L series					
	L1	L2	L3	L4	L5	L6
La_2O_3	1	2	3	4	5	10
	E series					
	E1	E2	E3	E4	E5	E6
Er_2O_3	1	2	3	4	5	10

crystallization peak temperatures for 1 h. The concentrations of rare-earth oxides in the samples are shown in Table 1.

The infrared (IR) spectra of the glasses were recorded at room temperature immediately after glass preparation by using the KBr disc technique. A Bruker IFS66V spectrometer was used to obtain the spectra in the wave number range of between 400 and 2000 cm^{-1} at a resolution of 2 cm^{-1}. DSC measurements were performed by a Netzsch STA449C calorimeter at a heating rate of 10 °C min^{-1}. For conducting thermal expansion measurements, specimens were prepared by polishing glass rods to dimensions of 5 mm × 5 mm × 20 mm and then tested in a Netzsch DIL402 dilatometer at a heating rate of 5 °C min^{-1}. The volume density was measured by the Archimedes method as the average value of three specimens for each glass. The Vickers hardnesses (H_v's) of the glasses were tested using a Wilson Wolpert 401MVD™ tester at a load of 300 g. Indentation was performed automatically at a predetermined dwell time of 5 s. The H_v's were calculated automatically according to the formula

$$H_v = \frac{0.1854P}{d^2}$$

where d is the average of two indentation diagonals in mm and P is the loading force in N. Five indents were used to obtain the mean value of H_v.

3. Results and discussion

3.1. Roles of rare-earth oxides in doped Bi_2O_3–B_2O_3 glass

The IR absorption spectra of the samples are shown in Fig. 1. Table 2 summarizes the major absorption bands and their vibration types. It is generally accepted that the two broad absorption bands observed at 900–950 cm^{-1} and 1200–1300 cm^{-1} are attributed to the stretching vibration of B–O–B in [BO_3] triangles [14,15] and the [BO_4] tetrahedron [16], respectively, and that the band observed at 680–720 cm^{-1} originates due to the bending vibration of B–O–B in [BO_3] triangles [14,15]. The band observed at 420–520 cm^{-1} is attributed to the vibration of Bi–O–Bi in the [BiO_6] octahedron [17–19]. Since the vibration band at 840 cm^{-1} [20] in [BiO_3] polyhedra is not clearly observed in the IR spectra, it is reasonable to consider that [BiO_6] is the main structural unit of the $Bi_2O_3{\cdot}2B_2O_3$ glasses.

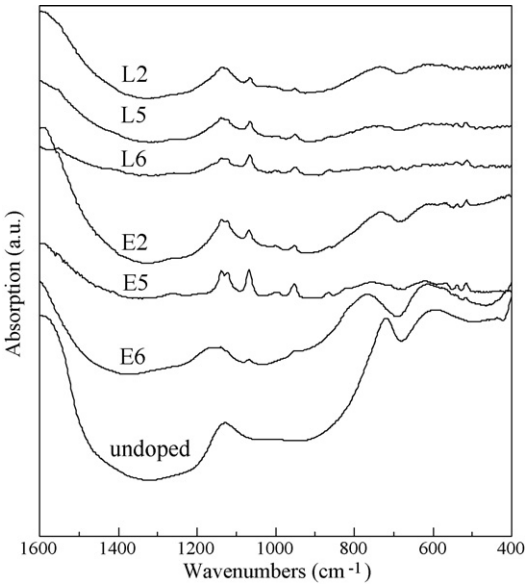

Fig. 1. Infrared absorption spectra of rare-earth oxides doped Bi_2O_3–B_2O_3 glasses.

As the doped concentration of rare-earth oxides is increased, the bands attributed to stretching vibration in the [BO_3] triangles seem to widen. This indicates the conversion of [BO_4] units to [BO_3] units. Since the addition of rare-earth oxides causes little change in the network structure of $Bi_2O_3{\cdot}2B_2O_3$ glass, it could be suggested that rare-earth oxides only act as network modifiers in the glass.

3.2. Dependence of glass stability on the concentration of rare-earth oxides

Characteristic temperatures including the glass transition temperature (T_g), crystallization temperature (T_p), and melting

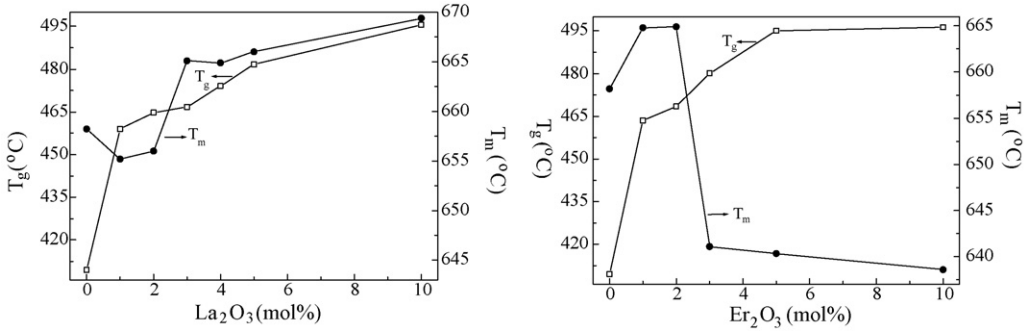

Fig. 2. The glass transition temperature (T_g) and the melting temperature (T_m) as a function of rare-earth oxide contents.

Table 2
Vibration types of the main absorption bands in the samples

Absorption bands (cm^{-1})	Vibration types
420–520	Vibration of Bi–O–Bi in [BiO_6] octahedron [17–19]
680–720	Bending vibration of B–O–B in [BO_3] triangles [14,15]
900–950, 1080	Stretching vibration in [BO_4] tetrahedron [16]
1200–1300	Stretching vibration of B–O–B in [BO_3] triangles [14,15]

temperature (T_m) are usually employed to estimate the stability of glass against crystallization. Fig. 2 shows the T_g and T_m values of the glasses, which are estimated using Proteus software installed in the DSC instrument. An increasing trend in T_g was observed in both the L series and E series; however, when the Er_2O_3 concentration is greater than 5 mol%, T_g remains almost the same. The higher T_g's of glasses doped with rare-earth oxides indicate that the structures of La_2O_3–Bi_2O_3–B_2O_3 glass and Er_2O_3–Bi_2O_3–B_2O_3 glass are more rigid in comparison with the structure of $Bi_2O_3{\cdot}2B_2O_3$ glass. It was observed that T_m slightly decreased at a La_2O_3 concentration of less than 2 mol%, but it increased at a higher La_2O_3 concentration. However, the relation between T_m and the Er_2O_3 concentration is opposite to that shown in Fig. 3(b). Thus, Er_2O_3 is favorable for decreasing the melting temperature of $Bi_2O_3{\cdot}2B_2O_3$ glass.

The DSC curves of the investigated glasses are shown in Fig. 3. Both the L series and the E series show higher crystallization temperatures than the crystallization temperature of undoped $Bi_2O_3{\cdot}2B_2O_3$ glass. As the rare-earth oxide concentration is increased, the crystallization temperature increases and the strength of crystallization peak decreases. This suggests that rare-earth oxides help to stabilize $Bi_2O_3{\cdot}2B_2O_3$ glass against crystallization. The large values of the ionic radii of the rare-earth ions in comparison with those of Bi^{3+} and B^{3+} may be the main reason for the increased resistance of $Bi_2O_3{\cdot}2B_2O_3$ glass to ion mobility and thermal diffusion, and consequently, for the prevention of nucleation and crystallization. The upper rare-earth oxides concentration (for which no exothermal peak was observed in doped $Bi_2O_3{\cdot}2B_2O_3$ glass during the heating process) of La_2O_3 (5 mol%) is much larger than that of Er_2O_3 (2 mol%). Therefore, Er_2O_3 is more effective than La_2O_3 for preventing the crystallization of $Bi_2O_3{\cdot}2B_2O_3$ glass.

Fig. 4 shows the XRD patterns of crystallized glasses that are heat treated at crystallization temperatures for 1 h. No crystals were observed in the L6 and E6 samples reheated at 600 °C for 4 h. The main crystal phase of the other samples is $Bi_6B_{10}O_{24}$. As the rare-earth oxide concentration is increased, the concentration of crystals decreases. Thus, the XRD results are consistent with the results of DSC analysis.

3.3. Effects of La_2O_3 and Er_2O_3 on physical properties

The thermal expansion coefficient (α) is one of the important factors that influence the refractive index of glass. The values of α at different concentrations of rare-earth oxides are illustrated in Table 3. As the rare-earth oxide concentration is increased, the α values of the doped glasses slightly decrease in comparison with the α value of undoped $Bi_2O_3{\cdot}2B_2O_3$ glass (9.05×10^{-6}/°C). The thermal expansion of a noncrystalline solid is controlled by the asymmetry in the amplitude of thermal vibrations in the material. The increase in the number of nonbridging bonds would weaken the glass structure and increase α. On the other hand, the decrease in the coordination

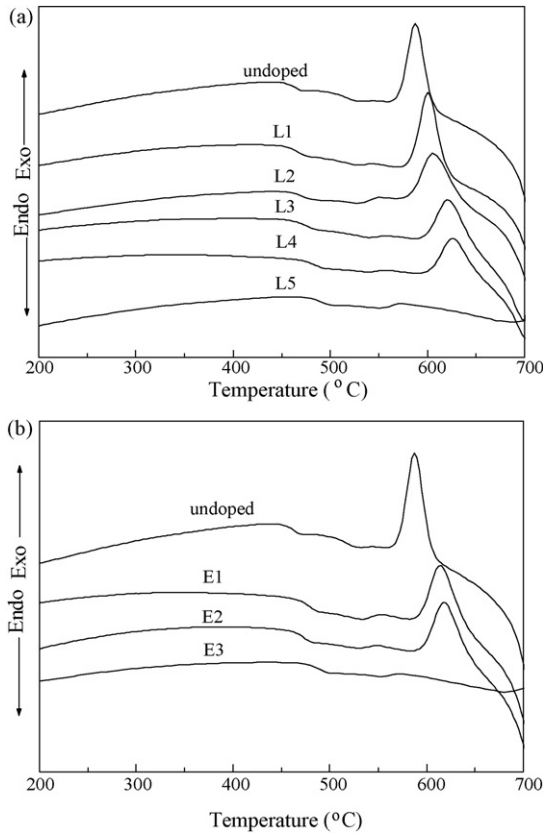

Fig. 3. DSC curves of different rare-earth oxide doped glasses (a) La_2O_3 doped; (b) Er_2O_3 doped.

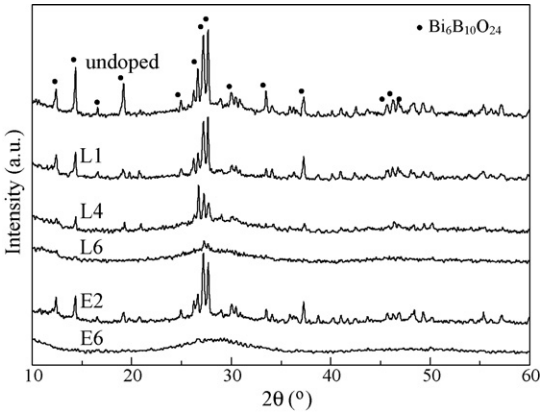

Fig. 4. XRD patterns of crystallized glasses heat-treated at around crystallization temperatures for 1 h.

Table 3
Thermal expansion coefficients of the samples ($\times 10^{-6}$/°C) (100–300 °C)

L series		
L3	L5	L6
8.93	8.85	8.72
E series		
E2	E4	E6
9.03	8.74	8.68

number of the network former may reduce α. The competition between the two opposing effects determines the change in α. The change from $[BO_4]$ to $[BO_3]$ is probably the dominant factor for reducing α. Lofaja et al. also reported a decrease in α for oxynitride glass doped with rare-earth oxides (including La_2O_3, Nd_2O_3, and Gd_2O_3) [21].

The density of a multicomponent material is commonly related to the density of each component in the material. Since both La_2O_3 (6.51 g/cm^3) and Er_2O_3 (8.64 g/cm^3) are heavier than $Bi_2O_3{\cdot}2B_2O_3$ glass (5.9 g/cm^3, as shown in Fig. 5), it may be suggested that the density of $Bi_2O_3{\cdot}2B_2O_3$ glass doped with rare-earth oxides should be larger than that of undoped glass. However, an opposite result was observed, as shown in Fig. 5. The different decrease amplitude of density between L series and E series may be understood by considering the difference between the values of the cationic field strengths of La^{3+} and Er^{3+}. The cationic field strength is a measure of a cation's effective force for attracting anions and is given by Z/r, where Z and r denote the valency and the ionic radius of the cation, respectively. Therefore, because Er^{3+} has a smaller ionic radius than La^{3+}, it has a larger cationic field strength, and accordingly, has a stronger ability to undergo coordination with other groups; this is possibly due to the formation of nonbridging bonds in the network structure. The increase in the number of nonbridging bonds would weaken the glass structure. Thus, when equal concentrations of Er^{3+} and La^{3+} are introduced in the glass, the density of Er_2O_3-doped glass would be smaller than that of La_2O_3-doped glass.

Microhardness is usually employed to estimate the surface vulnerability of glass and the difficulty in surface polishing.

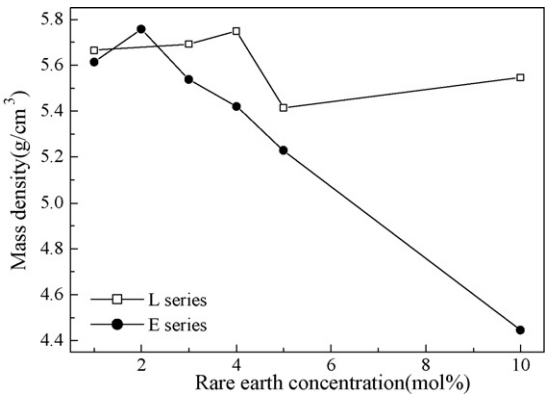

Fig. 5. Mass density as a function of rare-earth concentration.

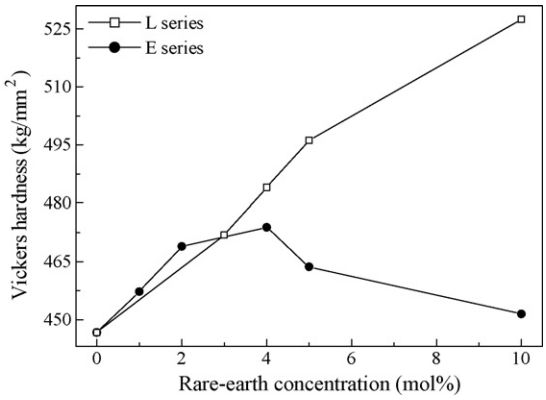

Fig. 6. Vickers hardness as a function of rare-earth oxide.

Fig. 6 shows the influence of the concentration of rare-earth oxides on H_v in $Bi_2O_3{\cdot}2B_2O_3$ glass. The highest value of H_v is obtained at a concentration of 4 mol% for Er_2O_3-doped glass. In contrast, H_v increases linearly with the La_2O_3 concentration. When the rare-earth ion lies in the interspaces of the glass network, it decreases the porosity of the glass host, and thereby increases the network connectivity; thus, the H_v value of the glass is increased. However, if the rare-earth ion disrupts the network units, it consequently decreases H_v. Since the number of nonbridging bonds in Er_2O_3-doped glass is probably more than that in La_2O_3-doped glass, the extent of crosslinkage in the glass structure of the latter would be greater and the H_v value would be higher. The highest value of H_v observed in Er_2O_3-doped glass suggests that the hardness of $Bi_2O_3{\cdot}2B_2O_3$ glass is not improved by overdoping it with Er_2O_3.

4. Conclusions

The addition of La_2O_3 and Er_2O_3 produces little change in the network structure of $Bi_2O_3{\cdot}2B_2O_3$ glass. As the doping concentration is increased, the crystallization temperature of the glass increases. When the concentrations of La_2O_3 and Er_2O_3 are greater than 4 and 2 mol%, respectively, the glasses become more thermally stable against crystallization. The decrease in the melting temperature due to the addition of Er_2O_3 will enable the increased use of the applications of $Bi_2O_3{\cdot}2B_2O_3$ glass at low temperatures. A suitable amount of La_2O_3 could tighten the glass network structure and improve the microhardness of $Bi_2O_3{\cdot}2B_2O_3$ glass.

References

[1] Y. Takahashi, Y. Benino, T. Fujiwara, T. Komatsu, J. Appl. Phys. 89 (2001) 5282.
[2] G. Senthil, K.B.R. Varma, Y. Takahashi, T. Komatsu, Appl. Phys. Lett. 78 (2001) 4019.
[3] Y. Takahash, Y. Benino, T. Fujiwara, T. Komatsu, J. Appl. Phys. 95 (2004) 3503.
[4] H. Hellwig, J. Leibertz, L. Bonhatŷ, J. Appl. Phys. 88 (2000) 240.
[5] R. Ihara, T. Honma, Opt. Mater. 27 (2004) 403.
[6] M. Eugenia, B. Bruno, G. Dominique, P. Guillaume, Nucl. Instrum. Meth. Phys. Res. A 537 (2005) 411.
[7] C.H. Kam, S. Buddhudu, Opt. Laser Eng. 35 (2001) 11.
[8] S.Q. Xu, Z.M. Yang, G.N. Wang, et al. J. Alloys Compd. 377 (2004) 253.

[9] M.B. Saisudha, J. Ramakrishna, Opt. Mater. 18 (2002) 403.
[10] T. Honma, Y. Benino, Opt. Mater. 20 (2002) 27.
[11] Y.J. Chen, Y.D. Huang, Opt. Mater. 25 (2004) 271.
[12] M.B. Saisudha, K.S.R.K. Rao, H.L. Bhat, J. Ramakrishna, J. Appl. Phys. 80 (1996) 4845.
[13] J.H. Yang, S.H.X. Dai, L. Wen, L.L. Hu, Z.H.H. Jiang, J. Appl. Phys. 93 (2003) 977.
[14] E.I. Kamitsos, A.P. Patsis, J. Non-Cryst. Solids 126 (1990) 52.
[15] A.K. Hassan, L. Borjesson, L.M. Torell, J. Non-Cryst. Solids 172/174 (1994) 154.
[16] G. El-Damrawi, K. El-Egili, Physica B 299 (2001) 180.
[17] Y. Dimitriev, M. Mihailova, in: Proceedings of the 16th International Congress on Glass, vol. 3, Madrid, 1992, p. 293.
[18] S. Hazra, S. Mandal, A. Ghosh, Phys. Rev. B 56 (1997) 13.
[19] M.E. Llines, A.E. Miller, K. Nassau, K.B. Lyons, J. Non-Cryst. Solids 89 (1987) 163.
[20] R. Iordanova, V. Dimitrov, Y. Dimitriev, D. Klissurski, J. Non-Cryst. Solids 180 (1994) 58.
[21] F. Lofaja, R. Sateta, M.J. Hoffmanna, A.R. de Arellano López, J. Eur. Ceram. Soc. 24 (2004) 3377.